INTERNATIONAL JOURNAL OF GEOMATICS AND GEOSCIENCES
Volume 2, No 2, 2011

Research article ISSN 0976 – 4380

Land use/Land cover changes in Hugli Estuary using Fuzzy C-Mean algorithm

Arun Mondal[1], Subhanil Guha[2], Prabhash Kumar Mishra[1], Sananda Kundu[1]
1- Research Scholar, Water Resources Development & Management, Indian Institute of Technology (IIT), Roorkee, Uttarakhand, India.
2- Assistant Professor, Department of Geography, Rammohan College, West Bengal, India
arun.iirs@gmail.com

ABSTRACT

In the present study, land use/land cover changes has been evaluated in the decade between 1989 and 2010 utilizing Landsat TM5 satellite images in the Hugli estuary which stretches across 4817.98 km^2 of Gangetic delta in West Bengal, India, predominantly dominated by mangrove plantation. The study utilizes supervised classification techniques using Fuzzy C-mean classification algorithm. The main advantage of this approach of classification is that no spectral information is lost like in the case of hard partitioning of feature space, thereby, generating a much accurate classified image. With an overall accuracy of 90% for 1989 image and 89% for 2010 image, and kappa coefficient of 0.87 and 0.85 for both images for 120 sample pixels; it can be said that this technique is very satisfactorily classifying the pixels into different features without losing any information. The total land area has been increased from 2007.63 km² (41.67%) in 1989 to 2159.39 km² (44.82%) in 2010, at an average rate of 7.23 km²/year. This is mainly due to the increased land area in the category of waste land and forest including mangrove plantation. This increase in land area is attributed to the huge deposition of silt through the silt-laden river networks in the region.

Keywords: Landsat TM5, Fuzzy C-mean, accuracy assessment, Kappa coefficient, mangrove plantation, transitional probability matrix etc.

1. Introduction

Hugli estuary is a very dynamic and complex land in term of changes. It is highly famous for “mangrove” vegetation. Mangroves are basically salt-tolerant plants of tropical and subtropical intertidal regions of the world. The particular regions where these plants grow are known as 'mangrove ecosystem'. These are highly productive but extremely sensitive and fragile. Experiences have proved that the presence of mangrove ecosystems on coastline save lives and property during natural hazards such as cyclones, storm surges and erosion. These ecosystems are also well known for their economic importance. They are breeding, feeding and nursery grounds for many estuarine and marine organisms. Hence, these areas are used for captive and culture fisheries. It is intersected by a complex network of tidal waterways, mudflats and small islands of mangrove forests, and presents an excellent example of ongoing ecological processes. The area is well known for its multi-range of flora and fauna.

Land use/land cover changes are very dynamic in nature and have to be monitored at regular intervals for sustainable development. For the evaluation of land use/land cover changes, the nature of change and the amount of change have to be determined through minute observation. The changes may be of natural or through human intervention. The recently developed techniques of Remote Sensing and Geographic Information System, nowadays, are playing an important role to determine the area and rate of changes.

Land use and land cover are two different terminologies that are very often used as a substitute of each other (Dimyati et al., 1996). "Land cover refers to the physical materials on the surface of a given parcel of land, while land use refers to the human activities that takes place on or make use of land e.g. residential, commercial, industrial etc (Longley et al., 2001)." According to Jensen (2007) who has investigated that urban landscape is a land use that is perceived as a way by which human beings utilize land while land cover exists as a natural environmental system (Jensen, 2007). Change detection in land use and land cover can be obtained on a temporal scale such as by considering decades to assess landscape change resulted due to anthropogenic activities on the land (Gibson and Power, 2000). These anthropogenic activities on land are the consequence of rapid urbanization and industrialization. Land use and land cover change have been recognized as significant drivers of global environment change (Turner et al., 1995).

Prakasam (2010) studied the land use and land cover change in Kodaikanal region of Western Ghats in Tamilnadu State of India for observing changes during a span of 40 years from 1969 to 2008 by using Landsat satellite data and performing supervised classification techniques (Prakasam, 2010). He found that 70% of the region was covered by forests in 1969 but has reduced to 33% in 2008; the built-up lands have increased from 3% to 21% depicting that the region is affected by rapid urbanization which is in turn leading to adverse environmental effects for the identified bio-diversity rich region of Kodaikanal. Samant and Subramanyam (1998) used Landsat TM imageries for studying the land use change in Bombay (Mumbai), India which is considered as the highest populated metropolis of India and found highly notable increase in built-up land by 300% and reduction in forest area by 55%, mainly due to the increasing pressure of urban expansion (Samant et al., 1998). He carried out a study by using land use maps of 1925 and 1967 and compared them with the Landsat imagery of 1994 for quantifying a change from 1925 to 1994.

Zubair (2006) used remote sensing and GIS technologies to detect the land use and land cover changes in Ilorin, Nigeria from 1972 to 2001 by Landsat TM images of 1972, 1986, and 2001. He has used Maximum likelihood algorithm of supervised classification method to delineate five land use and land cover classes for the study, namely: farmland, wasteland, forest, built-up and water-bodies (Zubair, 2006).

For the present study, supervised classification technique has been considered because the pixel categorization process is done after specifying the sample training areas. Each pixel in the data set is then compared numerically to each category in the interpretation key and labeled with the name of the category it most closely resembles if the pixel is insufficiently similar to any training data set; it is usually labeled "unknown". Actually, in the supervised approach we define useful information categories and then examine their spectral separability.

The present study has examined the land use and land cover of the area in the last two decades using multi-date remote sensing images. Then, attempt has been made to calculate and evaluate the change of land cover as a whole. The nature and pattern of change of delta and deltaic islands by the process of erosion and deposition has also been observed. Moreover, sophisticated supervised classification technique with fuzzy logic has been applied to get much more accurate result. Fruitfulness of transitional probability matrices regarding this study has also been examined. Finally, we can draw a conclusion that this classification technique is how much appropriate for this study area.

2. Study Area

The study was conducted in part of Hugli estuary, which stretches across 4817.98 km^2 of Gangetic delta in West Bengal, India. Some of the large and famous islands like Nayachara, Sagar and Ghoramara are situated in this dynamic area. The area, bounded geographically by $87^0$55'01"N to $88^0$48'04"N latitude and $21^0$29'02"E to $22^0$09'00"E longitude, is quite typical of the mangrove forest landscapes of deltaic West Bengal. It is also a center of economic activities, such as extraction of timber, fishing and collection of honey. The area experiences a subtropical monsoonal climate with an annual rainfall of 1600-1800 mm and severe cyclonic storms with the highest intensity of rainfall from June to September. Due to the monsoon, the total amount of rainfall in these four months account for more than half of the total amount of the yearly rainfall receiving in this area. The location map of the study area is shown in Figure 1.

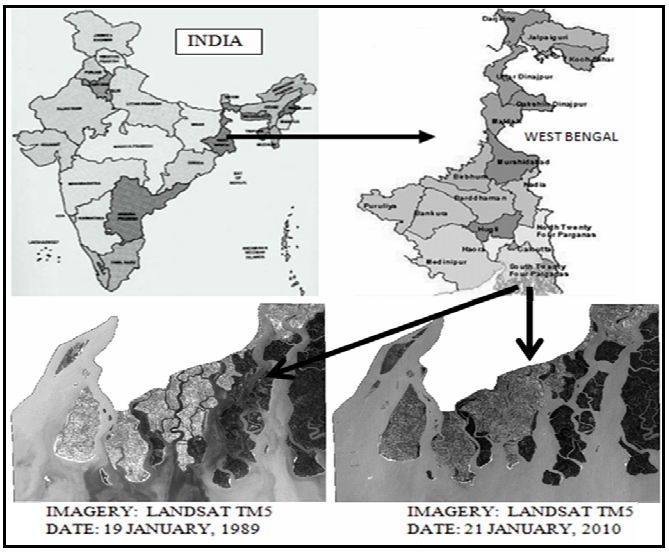

Figure 1: Study area along with Landsat TM satellite imageries

Topographically this area is under deltaic plain land which is still being developed. Enormous amount of sediments carried by the rivers contribute to its expansion and dynamics. Salinity gradients change over a wide range of spatial and temporal scales. The soil is more saline due to tidal inundation and therefore less fertile for the large scale production of food crops and other crops. The Sundarban mangroves lie on a delta that is relatively young geologically and has been undergoing drastic changes. These changes are caused by neotectonic activity that is causing the tilting of the delta towards the east, and by the enormous amounts of sediments transported by the rivers originating in the Himalaya. The accretion of sediments in the western part and the tilting to the east causes the river to migrate eastwards. Vegetation has typical tropical characteristics being mangrove is the leading special one. Actually mangrove forest consists of more than 75% of the total forest covered land in the study area. A very few settlements are found in the deltaic islands of the western part of the study area where the percentage of mangrove vegetation is comparatively less.

3. Data Used

Phenological variation could complicate consistency in image classification between scenes. We, therefore, selected cloud free images of 1989 (Landsat TM5) and 2010 (Landsat TM5) from winter season to analyze the actual landuse/landcover changes in the study area. The

Landsat TM5 data captured on 19 January, 1989 and 21 January, 2010 have been used in this study. A brief description of the used satellite images has been given in Table 1.

Table 1: Satellite data characteristics

Data Type	Acquisition Date	Path/Row	Sun Azimuth (°)	Sun Elevation (°)	Resolution (m)
LANDSAT TM5	19/1/1989	138/45	140.009792	36.905332	30
LANDSAT TM5	21/1/2010	138/45	143.935974	39.7974968	30
	Minimum/Maximum Radiance Value Table				
Acquisition Date		Band1	Band2	Band3	Band4
19/1/1989 ($L\max_{\lambda}$)		171	336	254	221
19/1/1989 ($L\min_{\lambda}$)		-1.52	-2.84	-1.17	-1.51
21/1/2010 ($L\max_{\lambda}$)		193	365	264	221
21/1/2010 ($L\min_{\lambda}$)		-1.52	-2.84	-1.17	-1.51
Minimum DN Value = 0; Maximum DN Value = 255					

4. Methodology

The present study attempts to examine the land use and land cover of the area in the last two decades using multi-date remote sensing images. Accordingly, land use/ land cover change detection has been done in the deltaic region of the Hugli estuary to calculate and evaluate the change of land cover in a whole. Observation has also been done to pin-point the nature and pattern of change of delta and deltaic islands by the process of erosion and deposition. For this, the present study utilizes remote sensing spatial data and topographical map available from various sources for different periods. Two images of the landsat TM5 with 30x30 m spatial resolution of 1989 and 2010 and topographical map with a scale of 1:50,000 are used. Prior to the assessment of land use/ land cover changes, these images are geo-referenced on the basis of rectified toposheet. Then, geometrically corrected images are calibrated for radiometric and atmospheric correction to minimize the error if any.

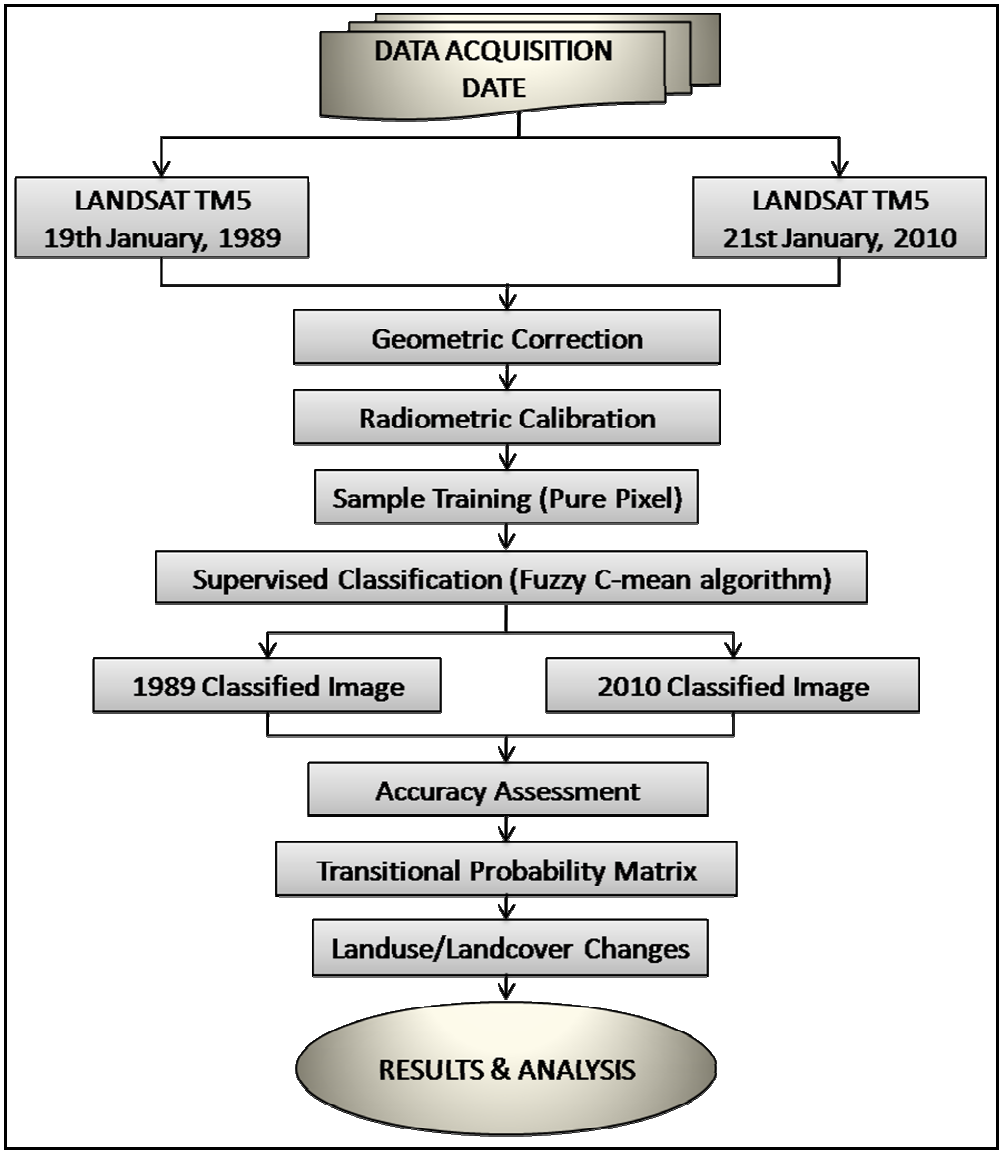

Figure 2: Flow Chart of Methodology

For the present study, supervised classification technique with fuzzy C-mean (FCM) fuzzy algorithm has been considered for generating land use/ land cover because the pixel categorization process is done after specifying the sample training areas. Each pixel in the data set is then compared numerically to each category in the interpretation key and labeled with the name of the category it most closely resembles if the pixel is insufficiently similar to any training data set; it is usually labeled "unknown". Before classification of the images pixel training and masking processes are performed.

After getting the classified images, classification accuracy of the images has been assessed through the methods of error matrix and transitional probability matrix. On the basis of producer accuracy, user accuracy, overall accuracy and kappa statistics the whole process of accuracy assessment has been done. Finally, after meeting the classification standards, the areal statistics of land use/ land cover changes in the study area are noted for analysis and also to get the end product of this study - the changed classified images of 1989 and 2010. All the processes of whole methodology, as discussed above, have been shown in a flow chart as given in Figure 2 above. Subsequent paragraphs, further discusses in details on the processes

of pre-processing of satellite data, image classification using C-mean fuzzy algorithm and accuracy assessment using error matrix and probability error matrix.

4.1 Pre-processing of Images

Pre-processing of satellite images include geometric correction, atmospheric correction, radiometric calibration and radiometric rectification procedures to facilitate comparability between dates (Jensen, 1996). The 1989 image was geometrically registered to 1:50,000 scale topographic maps; and 2010 image was geometrically registered to the 1989 base image. Root mean square errors of registration were maintained at 1 pixel (<30m) only.

After getting the geometrically corrected image the radiometric calibration and image rectification processes were run unless and until the rectified and corrected images were found.

At the first stage, DN value is converted into spectral radiance (L_λ) after checking the gain value using the official NASA approved ranges of $L\max_\lambda$ and $L\min_\lambda$ by the following formula (Chander and Grian, 2003; Melesse, 2004; & NASA, 2004):

$$L_{TOA} = \left(\frac{L\max_\lambda - L\min_\lambda}{QCAL\max - QCAL\min}\right) * (DN - QCAL\min) + L\min_\lambda \quad (1)$$

Where, $L\max_\lambda$ = maximum radiance (in $Wm^{-2}sr^{-1}\mu m^{-1}$); $L\min_\lambda$ = minimum radiance (in $Wm^{-2}sr^{-1}\mu m^{-1}$); $QCAL\max$ = maximum DN value possible (255); $QCAL\min$ = minimum DN value possible (0 or 1).

Radiance value is converted into reflectance using following equation (Schowengerdt, 2007):

$$\rho = \frac{L_{TOA}\pi d^2}{ESUN_\lambda \cos\theta_z} \quad (2)$$

Where, ρ = Reflectance; d^2 = Earth sun distance (AU); $ESUN_\lambda$ = Band dependent exoatmospheric irradiance $(Wm^{-2}\mu m^{-1})$; θ_z = Solar zenith angle (degree).

$$d = 1.001672 * \sin\left(\frac{2\pi(J - 93.5)}{356}\right) \quad (3)$$

Where, J = Julian day.

4.2 Classification of the Images

Supervised classification technique with fuzzy logic has been applied to classify both the images. The fuzzy concept of classification is a natural model in which each pixel may have partial membership to several land cover classes. It gives membership values for each sample for each class with the ranges between 0 and 1. In the present study, the fuzzy C-mean (FCM) algorithm is used for fuzzy clustering technique. This algorithm is developed based on iterative minimization of the following objective function:

$$J(U,V) = \sum_{i=1}^{C}\sum_{k=1}^{N} u_{ik}^{m} \left\| X_k - V_i \right\|^2 , \; 1 \le m \le \infty \tag{4}$$

Where, $X_1.....X_N$ are N data sample vectors; $V_1.....X_C$ are cluster centers; $U = [u_{ik}]$ is a C x N matrix, where u_{ik} is the i^{th} membership value of the k^{th} input sample X_k.

The membership values satisfy the following three constraints:

$$0 \le u_{ik} \le 1; \qquad i \in \{1,....,C\}, k \in \{1,....,N\} \tag{5}$$

$$\sum_{i=1}^{C} u_{ik} = 1; \qquad k \in \{1,....,N\} \tag{6}$$

$$\sum_{k=1}^{N} u_{ik} > 0; \qquad i \in \{1,....,C\} \tag{7}$$

The objective function is the sum of the square of the Euclidean distances between each input sample and its corresponding cluster center, with the distances weighted by the fuzzy memberships. The algorithm is iterative and makes use of the following equations:

$$V_i = \left[\sum_{k=1}^{N} u_{ik}^{m} X_k \right] / \sum_{k=1}^{N} u_{ik}^{m} \tag{8}$$

$$u_{ik} = 1 / \sum_{j=1}^{C} \left[\left\| X_k - V_i \right\| / \left\| X_k - V_j \right\| \right]^{2/(m-1)} \tag{9}$$

For calculation of a cluster center, all input samples are considered and the contributions of the samples are weighted by the membership values. For each sample, its membership value in each class depends on its distance to the corresponding cluster center. The weight factor m reduces the influence of small membership values. The larger the value of m, the smaller the influence of samples with small membership values (Clement, 2010).

4.3 Accuracy Assessment

It can be said that without accuracy assessment the classification process is incomplete. The accuracy of this classification has been assessed through error matrix or confusion matrix. Error matrices compare different categories of an automated classification with the known reference data or ground truth (Congalton and Green, 1999). These matrices are square, where the total number of rows and columns are equal to the number of different land use/land cover classes. This matrix stems from classifying the sampled training set pixels and listing the known cover types used for training (columns) versus the actual classified pixels (rows). Through the error matrices various classification errors of omission (exclusion) and commission (inclusion) have been studied. Omission errors and commission errors are represented by no-diagonal column elements and row elements respectively as shown in Table-2 and Table-3. The overall accuracy is computed by dividing the total number of correctly classified pixels by the total number of reference pixels. Producer's accuracies are calculated by dividing the number of correctly classified pixels in each category by the number of training set pixels used for that category. User's accuracies are computed by dividing the number of correctly classified pixels in each category by the total number of pixels that were classified in that category.

4.4 Kappa Coefficient

In the present study Kappa coefficient has been applied for accuracy assessment which is nothing but a discrete multivariate technique. Kappa analysis yields *Khat statistic* that is the measure of agreement of accuracy. The *Khat statistic* is computed as (Lillesand and Kiefer, 2000):

$$Khat = \frac{N\sum_{i=1}^{r} X_{ii} - \sum_{i=1}^{r}(X_{i+} \times X_{+i})}{N^2 - \sum_{i=1}^{r}(X_{i+} \times X_{+i})} \quad (10)$$

Where, r = the number of rows in the error matrix; X_{ii} = the number of observations in row 'i' and column 'i' (on the major diagonal); X_{i+} = total of observations in row 'i' (shown as marginal total to right of the matrix); X_{+i} = total of observations in column 'i' (shown as marginal total at bottom of the matrix); N = the total number of observations included in matrix.

4.5 Transitional Probability Matrix

A transitional probability matrix is calculated by dividing the frequency of transitions n_{ij} by the frequency of state $i(n_{ij/} n_{i+})$. Therefore it represents a conditional probability, the probability to move to state *'j'*, provided that the subject is in state *'i'*. The transitional probability differs from the joint probability, which reflects the overall probability for observing a certain transition (it is calculated by dividing n_{ij} by the total number of observations *N*). Analysis of a transitional probability matrix is undertaken row by row, as one may investigate the most and least frequent transitions with a transitional frequency matrix, as accounted by the highest and lowest row percents.

There are some limits to transitional probability matrix method. For less frequent states, transitional probabilities tend to be "artificially" high. Another limit is related to the descriptive aspect of the transitional probability matrix and these are only "raw numbers".

Transitional probability matrices are the first mathematical operations an investigator should perform while analyzing the dynamics of categorical data. They show information regarding the underlying structure of the data sequence. One should analyze the matrix by examining the most and least frequent transitions, either from a row by row or in a column by column sequence.

5. Results and Discussion

Once the images for the year 1989 and 2010 are classified through supervised classification technique using C-mean fuzzy algorithm, we applied error matrices to assess the accuracy of classification. Kappa coefficient (*Khat statistic*) is also applied in this study. Further, transitional probability matrices are very helpful to get the correct result. Areal statistics of land use/land cover changes has also been shown graphically in Figure 3 and Figure 4 respectively. After getting the classified images, the statistics of some sample pixels of band1, band2, band3 and band4 for both the images are obtained. Minimum, maximum, mean, median, mode and standard deviation values have been evaluated from the sample pixels as

given in Table 2. For example; for a sample area under mangrove forest in 1989 classified image, the minimum and maximum values of those pixels for band1, band2, band3 and band4 are 67, 27, 23 & 52 and 73, 30, 27 & 63 respectively. For the same sample pixels in 2010 classified image, the minimum and maximum values for band1, band2, band3 and band4 are 59, 25, 21 & 54 and 65, 29, 24 & 62 respectively (Table 2). It shows a very good result for the classified images.

For accuracy assessment, a total of 120 sample points are randomly taken from each images covering different classes. The error matrices of 1989 and 2010 images have been given in Table 3 and Table 4 respectively. From the tables of error matrix the values of producer accuracy and user accuracy are obtained and on the basis of these values the values of overall accuracy and kappa coefficient have been determined. The error matrix for 1989 image indicates an overall accuracy of 90%. Producer's accuracies range from 86% (water body) to 100% (settlement) and user's accuracies vary from 80% (agricultural land) to 100% (settlement). Value of kappa coefficient is 0.87 as given in Table-3.

The error matrix for 2010 image represents an overall accuracy of 89%. Producer's accuracies range from 80% (wasteland) to 100% (settlement) and user's accuracies vary from 77% (agricultural land) to 100% (settlement). Value of kappa coefficient is 0.85 as given in Table 4. Transitional Probability Matrix analyzes the most and least frequent transitions, either from a row by row or a column by column fashion and is presented in Table-5.

Table 2: Samples statistics of land use/land cover types in different bands

Class Name	Sample Statistics	1989				2010			
		band1	band2	band3	band4	band1	band2	band3	band4
Water	Min	73.00	28.00	19.00	10.00	79.00	36.00	28.00	12.00
	Max	79.00	30.00	22.00	12.00	85.00	39.00	31.00	14.00
	Mean	76.19	28.92	20.91	10.98	82.16	37.02	29.61	12.93
	Median	76.00	29.00	21.00	11.00	82.00	37.00	30.00	13.00
	Mode	76.00	29.00	21.00	11.00	82.00	37.00	30.00	13.00
	Std. Dev	1.09	0.46	0.49	0.28	1.10	0.49	0.67	0.42
Wasteland	Min	122.00	60.00	72.00	64.00	96.00	50.00	60.00	68.00
	Max	134.00	69.00	80.00	73.00	116.00	62.00	74.00	72.00
	Mean	128.94	64.75	76.69	70.13	105.19	54.81	66.38	70.25
	Median	129.00	64.00	76.00	70.00	105.00	54.00	66.00	70.00
	Mode	129.00	64.00	79.00	69.00	103.00	54.00	66.00	70.00
	Std. Dev	3.80	2.75	2.47	2.06	5.04	2.99	3.18	1.13
Mangrove	Min	67.00	27.00	23.00	52.00	59.00	25.00	21.00	54.00
	Max	73.00	30.00	27.00	63.00	65.00	29.00	24.00	62.00
	Mean	69.40	28.80	25.31	57.89	61.65	27.52	22.61	58.50
	Median	69.00	29.00	25.00	58.00	62.00	28.00	23.00	59.00
	Mode	70.00	29.00	26.00	57.00	62.00	28.00	23.00	59.00
	Std. Dev	1.15	0.53	0.76	1.83	1.10	0.64	0.60	1.48
Forest	Min	71.00	30.00	30.00	43.00	64.00	28.00	28.00	38.00
	Max	77.00	32.00	32.00	50.00	70.00	32.00	32.00	42.00
	Mean	73.91	31.55	30.24	47.24	67.10	29.29	29.64	39.19
	Median	74.00	32.00	30.00	47.00	67.00	29.00	29.00	39.00
	Mode	73.00	32.00	30.00	49.00	67.00	29.00	29.00	39.00
	Std. Dev	1.23	0.55	0.48	2.03	1.45	0.81	0.96	0.89
Agriculture	Min	83.00	37.00	41.00	47.00	75.00	37.00	44.00	49.00
	Max	88.00	40.00	44.00	50.00	80.00	39.00	46.00	53.00
	Mean	85.36	38.48	42.24	48.60	77.28	37.48	44.84	51.36

	Median	85.00	38.00	42.00	49.00	77.00	37.00	45.00	51.00
	Mode	85.00	38.00	42.00	49.00	77.00	37.00	45.00	51.00
	Std. Dev	1.32	0.65	0.72	0.65	1.21	0.59	0.55	1.15
Settlement	Min	74.00	30.00	28.00	41.00	63.00	27.00	24.00	24.00
	Max	81.00	36.00	37.00	49.00	73.00	34.00	37.00	56.00
	Mean	75.93	31.36	29.54	45.82	67.00	29.00	27.11	48.93
	Median	76.00	31.00	29.00	46.00	67.00	29.00	26.00	49.00
	Mode	76.00	31.00	28.00	47.00	67.00	28.00	26.00	50.00
	Std. Dev	1.33	1.22	1.99	2.09	2.23	1.41	2.53	3.84

Table 3: Error Matrix (1989)

Class Name	Reference Total	Classified Total	Number of Correct Points	Producers Accuracy (%)	Omission Error (%)	Users Accuracy (%)	Commission Error (%)
Water Body	14	13	12	0.86	0.14	0.92	0.08
Waste Land	13	13	12	0.92	0.08	0.92	0.08
Mangrove Forest	45	46	41	0.91	0.09	0.89	0.11
Forest	33	31	29	0.88	0.12	0.94	0.06
Agriculture	13	15	12	0.92	0.08	0.80	0.20
Settlement	2	2	2	1.00	0.00	1.00	0.00
Total	120	120	108	-	-	-	-
Overall Accuracy = 90%, Kappa Khat = 0.87							

Table 4: Error Matrix (2010)

Class Name	Reference Total	Classified Total	Number of Correct Points	Producers Accuracy (%)	Omission Error (%)	Users Accuracy (%)	Commission Error (%)
Water Body	13	12	11	0.85	0.15	0.92	0.08
Waste Land	15	13	12	0.80	0.20	0.92	0.08
Mangrove Forest	47	51	44	0.94	0.06	0.86	0.14
Forest	32	29	28	0.88	0.13	0.97	0.03
Agriculture	11	13	10	0.91	0.09	0.77	0.23
Settlement	2	2	2	1.00	0.00	1.00	0.00
Total	120	120	107	-	-	-	-
Overall Accuracy = 89%, Kappa Khat = 0.85							

Table 5: Transitional Probability Matrix

Year 1989			Year 2010				
Land use/Land	Water Body	Waste Land	Mangrove Forest	Forest	Agriculture	Settlement	Total

Cover							
Water Body	2594.77	107.94	86.435	21.03	0.17	0.001	2810.35
Waste Land	21.86	194.31	22.04	84.98	50.46	5.19	378.85
Mangrove Forest	28.07	30.11	831.813	49.84	3.08	3.09	946.00
Forest	11.70	69.79	50.73	333.85	13.08	2.51	481.66
Agriculture	2.17	44.30	2.23	24.95	118.85	2.41	194.91
Settlement	0.01	0.00	0.00	0.00	0.00	6.19	6.20
Total	2658.58	446.45	993.25	514.65	185.64	19.39	4817.97

The temporal changes of land use/land cover in the study area are illustrated in Figure 3. The classified satellite images for the study area are shown in Figure 4. The estimated land area has been increased from 2007.63 km² (41.67%) in 1989 to 2159.39 km² (44.82%) in 2010, at an average rate of 7.23 km²/year. From 1989 to 2010, the net area under forest, mangrove forest and waste land were slightly increased at the rate of 0.68%, 0.98% and 1.41% respectively. The region can be attributed as a great example for researchers to study on the mangrove forest ecosystem due to its predominant mangrove forest cover. The area under forest including mangrove forest includes 29.64% in 1989 and 31.30% in 2010. There was a net gain of 80.23 km² of forest area (including mangrove forest and other forest), and the annual rate of increase was 3.82 km²/year. This increase is mainly due to increasing deposition of silt through particle laden river networks. The detail on the areal statistics of land use/ land cover is given below in Table 6.

Table 6: Areal Statistics of Land use/Land Cover

Land use/Land Cover	Assessment for the year 1989		Assessment for the year 2010	
	Area in km²	% coverage	Area in km²	% coverage
Water Body	2810.35	58.33	2658.59	55.18
Waste Land	378.85	7.86	446.45	9.27
Mangrove Forest	946.01	19.64	993.25	20.62
Forest	481.66	10.00	514.65	10.68
Agriculture	194.91	4.05	185.65	3.85
Settlement	6.20	0.13	19.40	0.40
Total	4817.98	100	4817.98	100

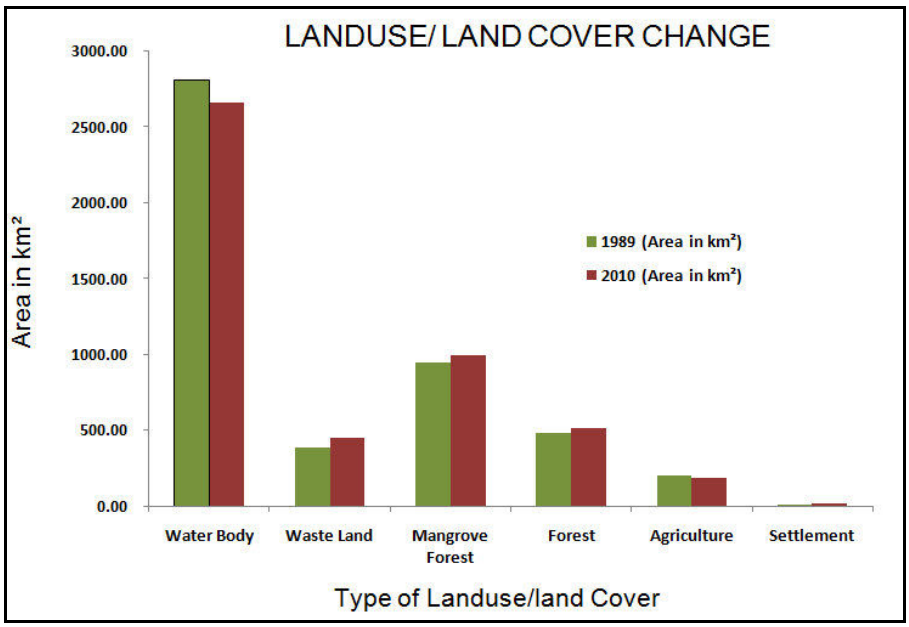

Figure 3: Temporal changes of Land use/Land cover in the study area

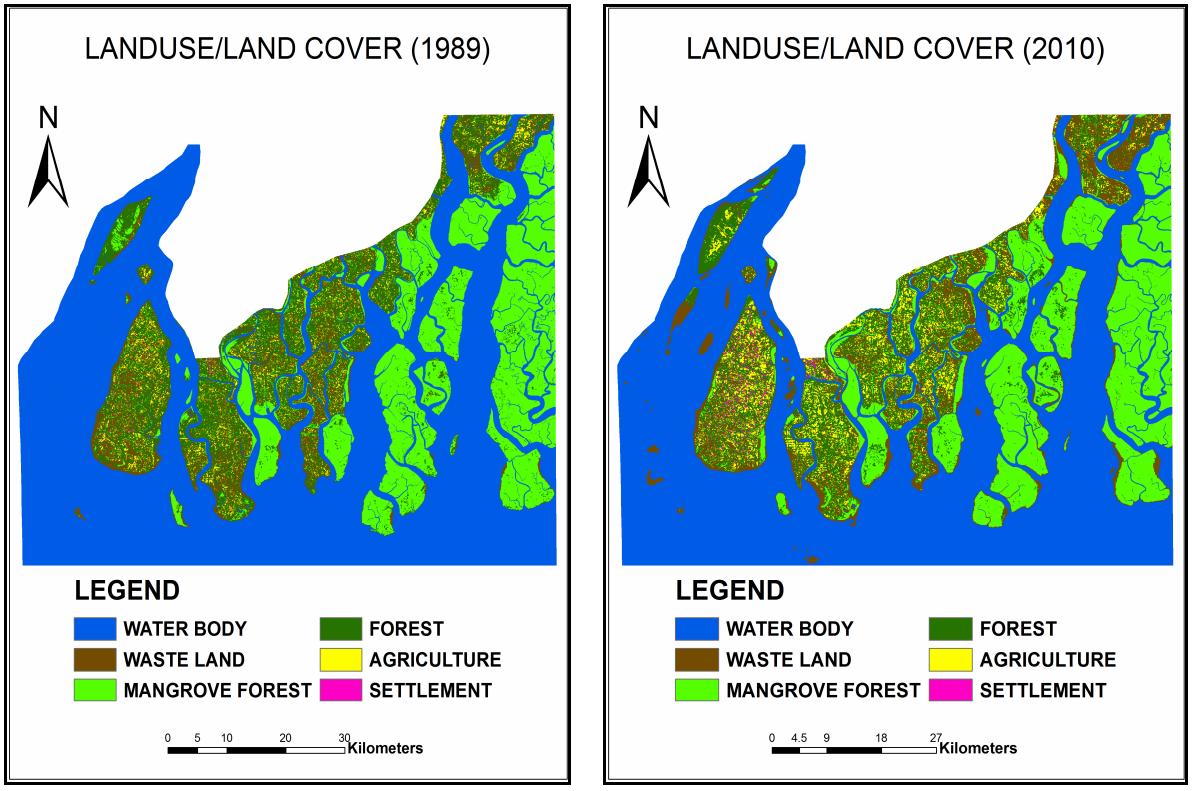

Figure 4: Classified landsat TM5 images for the year 1989 and 2010

5.1 Conclusion

In this paper, Landsat TM5 Satellite images of 1989 and 2010 has been utilized to assess the decadal land use/ land cover changes in the in Hugli estuary, West Bengal. For this, the two images were classified through supervised classification techniques using Fuzzy C-Mean (FCM) classification algorithm, which has the advantage of no losses in the spectral information of features in comparison to other classification methods. With an overall accuracy of 90% for 1989 image and 89% for 2010 image, and kappa coefficient of 0.87 and

0.85 for both images for 120 sample pixels; it can be said that this technique is very satisfactorily classifying the pixels into different features without losing any information quite accurately. Examination of sample statistics also supports this result (Table-2). The total land area has been increased from 2007.63 km² (41.67%) in 1989 to 2159.39 km² (44.82%) in 2010, at an average rate of 7.23 km²/year. Hence, an increase of 151.76 km² net land area mostly due to increased wasteland and forest including mangrove has been witnessed in the region. This is mainly due to silt deposit in the region due to particle laden river networks. However, we need to ascertain whether this rate is increasing or decreasing through analyzing more number of satellite images between 1989 and 2010 to get the actual changing rate. It is a land where erosion and deposition is taking place at alarming rate, thereby, it can be concluded that this geomorphologically active landscape will further change extensively in coming days.

Acknowledgement

The authors, thankfully, acknowledges the help and support rendered by Dr. D. N. Das, Asst. Prof., School of Social Science, Jawaharlal Nehru University, New Delhi during the study period. We are also thankful to the The Global Land Cover Facility (GLCF) centre for providing quality satellite images without which study would not have been made possible. Lastly, we acknowledge our thankfulness to Survey of India, Dehradun, India for procuring topographical maps which are used as the reference maps in the study.

6. References

1. Chander, G., and Grian L.M (2003), "Revised Landsat-5 TM Radiometric Calibration Procedures and post-calibration Dynamic Ranges", IEEE Transactions on geosciences and remote sensing, 41(11), pp 2674-2677.

2. Clement, E.A., Sumith, P., Serwan, B., and Daniel, B (2010), "Modeling Methane Emission from Wetlands in North-Eastern New South Wales, Australia Using Landsat ETM+", Remote Sensing, 2(5), pp 1378-1399.

3. Congalton, R.G., and Green, K (1999), "Assessing the accuracy of remotely sensed data: principles and practices", Lewis Publishers, Boca Raton.

4. Dimyati, M., Mizuno, K., and Kitamura, T (1996), "An Analysis of Land Use/Cover Change using the combination of MSS Landsat and Land Use Map: A Case Study in Yogyakarta, Indonesia", International Journal of Remote Sensing, 17(5), pp 931-944.

5. Gibson, P., and Power, C (2000), "Introductory Remote Sensing: Digital Image Processing and Applications", Routledge, pp 92-112.

6. Jensen, J.R (1996), "Introduction to Digital Image Processing: A Remote Sensing Perspective", Englewood Cliffs, New Jersey: Prentice-Hall.

7. Jensen, J (2007), "Remote Sensing of the Environment: An earth Resource Perspective", Pearson Education, Inc. Secondnd Edition, pp 450.

8. Lillesand, T.M., and Kiefer, R.W (2000), "Remote Sensing and Image Interpretation", John Wiley & Sons, Inc, pp 572-576.

9. Longley, P., Donnay, J., and Barnsley, M (2001), "Remote Sensing and Urban Analysis", Taylor and Francis, London, (eds.) pp 117.

10. Melesse, A.M (2004), "Spatiotemporal dynamics of land surface parameters in the Red river of the north basin". Physics and Chemistry of the Earth. 29, pp 795-810.

11. NASA (2004), "Landsat 7 Science Data Users Handbook, Landsat Project Science Office", Chapter 11-Data Products.

12. Prakasam, C (2010), "Land use and land cover change detection through remote sensing approach: A case study of Kodaikanal Taluk, Tamilnadu", International Journal of Geomatics and Geosciences, (1-2), pp 150-158.

13. Samant, H.P., and Subramanyam, V (1998), "Landuse/Land Cover Change in Mumbai-Navi Mumbai Cities and Its Effects on the Drainage Basins and Channels – A Study Using GIS", Journal of the Indian Society of Remote Sensing, 26, (1&2), pp 1-6.

14. Schowengerdt, R.A (2007), "Remote Sensing: Models and Methods for Image Processing", Elsevier publication, Third Edition, pp 442-445.

15. Turner.B., Skole.D., Sanderson.S., Fisher.G., Fresco.L., and Leemans.R (1995), "Land Use and Land Cover change Science/Research Plan, International. Human Dimensions of Global Environmental Change Programme (IHDP)", Report No. 07 (http://www.ihdp.uni-bonn.de/html/publications/reports/report07/luccsp.html# Executive).

16. Zubair, A (2006), "Change Detection in Land Use and Land Cover using Remote Sensing Data and GIS: A Case Study of Ilorin and its Environs in Kwara State", GIS Development Journal. (http://www.gisdevelopment.net/thesis/ OpeyemiZubair_ ThesisPDF.pdf)